

Material properties of CMT—metal additive manufactured duplex stainless steel blade-like geometries

Gerhard Posch¹ · Kerstin Chladil² · Harald Chladil³

Received: 17 October 2016 / Accepted: 11 April 2017 / Published online: 17 May 2017
© International Institute of Welding 2017

Abstract Impeller blades are often individual and complex-shaped components made of challenging metals. As the manufacturing of such blades is highly sophisticated, only a few companies worldwide possess the necessary processing knowledge and that is why long production times have to be accepted by customers. To overcome this economic disadvantage, manufacturing technologies are permanent under supervision and it seems that metal additive manufacturing could thereby play an important role in future. In this paper, wire arc additive manufacturing (WAAM) based on gas metal arc welding (GMAW) is considered. Shape-giving GMAW is well known in industrial manufacturing, but its application is limited due to restrictions by the welding process itself: For thinner wall thicknesses, a significant reduction of the weld process energy is required which increases the risk of process instabilities and spatter formation. Extensive welding process-related efforts have been undertaken to overcome this fact and a new GMAW process, called CMT (Cold Metal Transfer) was introduced. CMT is based on a high-frequency forward and backward movement of the welding wire electrode and provides an almost spatter-free and absolute precise, periodic detachment of accurately defined droplets from the filler wire at very low process energies. In combination with an accurate

robotic movement of the CMT welding torch, geometries with minimum thicknesses in the range of 2–4 mm can be build up layer by layer. Additionally, a broad range of different, well established and third party-approved GMAW filler metals for joining is available. In this work, an impeller blade-like geometry out of duplex stainless steel has been manufactured by CMT using a filler wire type G 22 9 3 N L. The investigations have shown that the achieved surface roughness is comparable to sand casting and the microstructure is without any evidence for porosity and lack of fusion. Furthermore, an austenite/ δ -ferrite weld microstructure with partly preferred grain orientations and a δ -ferrite content of around 30FN exists. The measured mechanical properties, especially strength and toughness, are comparable to data provided by the filler metal data sheet.

Keywords (IIW Thesaurus) Gas Metal Arc-Welding (GMAW) · Cold Metal Transfer (CMT) · Duplex Stainless Steel, G 22 9 3 N L · ER2209 · Additive Manufacturing (AM) · Wire Arc Additive Manufacturing (WAAM)

1 Introduction

Additive manufacturing, originally called 3D–printing, is currently one of the most emerging engineering topics. Already in the early 1980s, first attempts on polymer models were created out of so-called 3D–printers by photopolymerisation of special polymers. Meanwhile, the processes in the field of polymers are remarkable improved, various types of polymers have been developed, and 3D prints of complicated customized parts are realized. Latest developments are customized dental braces made of degradable photopolymers by UV based additive manufacturing [1].

Recommended for publication by Commission I - Additive Manufacturing, Surfacing, and Thermal Cutting

✉ Gerhard Posch
posch.gerhard@fronius.com

¹ Fronius Int., Wels, Austria

² Materials Center Leoben, Leoben, Austria

³ Andritz AG, Graz, Austria

However, for engineering purposes, often metallic components are required and research focuses now also on metal additive manufacturing. Here, the main approach is a precise localized sintering or melting of metal powder in a layer by layer technique with a laser or an electron beam. With this so-called “powder bed process” very complex shaped and even hollow metallic parts can be established. Nevertheless, they are restricted in their maximum achievable size and thicknesses due to economic factors as a rather low build-up rate, expensive equipment, and high powder costs. For bigger 3D-shaped components like wings, turbine plates and valves, economic considerations are more dominant and it is necessary to reduce the additive manufactured component costs by, e.g., replacement of the more expensive powder by a less expensive wire and the reduction of the manufacturing equipment costs by use of a cheaper heat source. Thus, a process where a wire is precisely melted down by an electric arc—wire arc additive manufacturing (WAAM)—may reach great economic importance. The interesting processes therefore are plasma arc and gas metal arc welding in combination with a “layer-by-layer” manufacturing technique [2].

2 “Shape-giving” GMAW process

GMAW is worldwide the most common used process for welding of metals. Thereby, a filler wire electrode is melted down by an electric arc and the weld groove is filled up with liquid metal. After its solidification, it is called “weld seam” and stands for a strong joint. But this process can also be used to establish overlays if the weld seams are arranged side by side and by laying seams over the others 3D structures can be build up. The accuracy of the 3D structures is thereby determined by the precision of the metal transfer and the robotic guidance of the welding torch. Such a technology, so-called MicroGuss™, was already successfully introduced in the early 1990s as an alternative manufacturing method for hydropower Pelton runners due to the bad availability and improvable reliability of fully cast Pelton runners [3]. The buckets are build up layer-by-layer by a shape-giving GMAW welding process on a central forged disc which contains only the bucket sockets. Beside this unique manufacturing technique, the metallurgical constitution

resulting in distinct mechanical properties are of great interest. The base metal is a low carbon, soft martensitic steel with 13% Chromium and 4% Nickel with very high toughness and strength requirements. Additionally, a porous-free material is a main criterion for this application. Using MicroGuss™, it is possible to manufacture technological approved Pelton runners in much shorter time (30% less) compared to fully cast runners. Moreover, this production technology has a further economic advantage especially in the production of smaller sized runners due to less material which has to be removed by the final milling operation. It could also be shown, that the mechanical behavior in critical areas within the runner is enhanced compared to cast structures. Till now, more than 400 runners have been built using this technology, acting more than 9 million service hours without any remarkable complaints [3].

3 CMT process

As shown in this successful example of WAAM based on GMAW, the main limitations are the minimum achievable wall thickness and a very rough sidewall surface. The “Cold Metal Transfer” (CMT) process [4–6], a further development of the GMAW short arc process, can improve these limitations due to its process-related characteristics. And as it can be combined with almost any available robot system, it is in a very powerful position for WAAM.

CMT was originally invented for joining steel to aluminum [4, 5, 7] which requires a very low heat input. To minimize the heat input the arc burning time is reduced to a minimum, just enough to melt the wire and to surface-fuse the base metal. In addition, the wire electrode is mechanically moved forward and backward at a high frequency by a secondary wire feeder, integrated in the torch, to support the droplet detachment during welding (Fig. 1). Frequencies up to 150 Hz guarantee thereby a very smooth, almost spatter-free droplet detachment, accompanied by a very short arc burning time which is also very beneficial for low dilution overlay welding [8].

Simple shapes like vases, ashtrays, or artistic objects made of various metals like aluminum, stainless steel, or bronze (Fig. 2) are made to demonstrate that CMT is highly capable in generating 3D objects. However, also more application-

Fig. 1 Principle of CMT: high-frequency forward and backward movement of the wire electrode

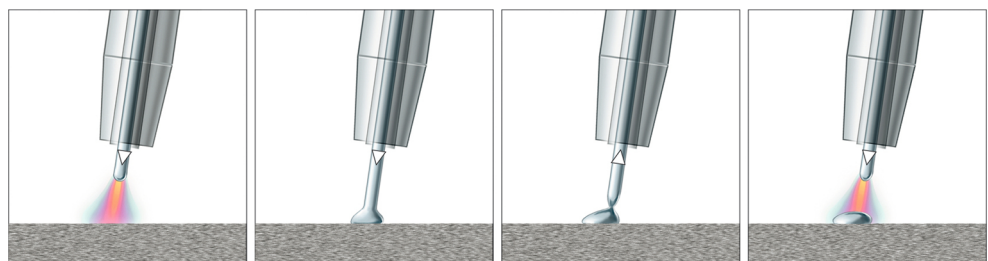


Fig. 2 CMT–MAM examples for thin-walled simple 3D–shapes out of different filler wires (unalloyed steel, stainless steel, aluminum, copper alloy)



related components (wing spars, wings, truncated cones) out of different metals are already established [9].

The realizable wall thicknesses are mainly determined by the welding heat input: the lower the heat input, the smaller the minimum achievable wall thickness. Additionally, they are influenced by the diameter of the filler wire, the wire feeding rate, and the filler metal alloy. Generally, the thinnest CMT-achievable wall thickness is in the range of 4–5 mm with a \varnothing 1.2-mm welding filler wire and around 2–4 mm based on a \varnothing 0.8-mm filler wire. On the other hand, thicker walls can simply be established by additional torch oscillation, higher wire feeding rates or different welding processes, e.g., modified pulse modes or spray arc modes [10]. Very thick walls can be fabricated by twin wire processes, e.g., CMT Twin [4, 5], or weld overlaying.

4 WAAM impeller blade-like geometries made by CMT

WAAM objects are often created for demonstration purposes and only less attention is paid to their mechanical properties. But to take WAAM into consideration as a real alternative for practical applications, the knowledge about the mechanical properties of WAAM parts is mandatory. That is why impeller plate-like geometries made of duplex stainless steel

were considered and investigated in this study. Nevertheless, there was also an economic driving force for this study: Due to the shape complexity, the state-of-the-art production method is casting and in combination with the demanding duplex stainless steel the pool of manufacturers is rather limited and very long delivery times are obligatory. This limits economic optimization and supply chain management. Thus, additive manufacturing could be a powerful tool for reducing delivery times and additionally enlarging the freedom of the designer for further improvement of the impeller's efficiency.

To figure out the capabilities of CMT in respect to achievable deposition rates, surface condition, wall thicknesses, inclination of walls and mechanical properties, blade-shaped geometries with comparable wall thicknesses to real impeller blades were CMT-welded by a robot layer-by-layer using a standard duplex stainless steel filler wire (Fig. 3).

4.1 Manufacturing data of WAAM blade-shaped geometry

The blade-like geometries were established using a Fronius TPS 4000 CMT on a robot and a duplex stainless steel filler wire in diameter 1.2 mm. The blades were built up on a horizontal mounted unalloyed steel base plate, and the decline from the vertical was achieved by a 0.5-mm horizontal

Fig. 3 WAAM duplex stainless steel blade-shaped geometry for technological evaluation; *left*: front view; *right*: side view



Table 1 Characteristic as-welded mechanical properties of all weld metal Thermanit 22/09, taken from the data sheet [11]

Yield strength ($R_{p0,2}$)	510 MPa
Yield strength ($R_{p1,0}$)	550 MPa
Tensile strength (R_m)	700 MPa
Elongation (A, $L_0 = 5d_0$; $d_0 = 10$ mm)	25%
Impact toughness (CVN, 20 °C)	70 J

sideward adjustment of the torch after each layer. The blades (Fig. 3) had a dimension of around $200 \times 220 \times 10$ mm.

The welding parameters were kept constant for all layers: the wire feed rate was set to 4.2 m/min, the welding speed was 36 cm/min. The amperage was 145 A, the voltage 11.9 V, and the CMT frequency was 100 Hz. As shielding gas Ar + 2.5%CO₂ was used. Additionally, the CMT torch oscillated 8 mm at a frequency of 2 Hz.

Before welding, the interpass temperature was always checked with a temperature measuring device. Welding was started when the temperature, in welding called “interpass temperature,” was below 150 °C-based on the recommendation of the filler metal supplier.

The total welding time for the buildup of 136 layers was 87 min, including interpass cooling times to prevent an overheating of the already “welded” part. The overall deposition rate was 1.7 kg/h.

To establish a much more vertical curved plane the base plate has to be additionally moved on a turntable which requires more sophisticated programming efforts for the combined movements of torch and turntable but this was not considered in this study.

A $\varnothing 1.2$ -mm filler wire, classified as G 22 9 3 N L according to EN ISO 14343-A, SS2209 according to EN ISO 14343-B and ER2209 according to AWS A5.9, was

used. Additionally, this wire was also certified by notable third parties [11]. The mechanical properties, shown in Table 1, are taken from the data sheet and valid for the as welded, all weld metal. The delta ferrite content of the all weld metal was said to be between 30 and 60 FN.

It has to be taken into account, that a filler metal data sheet is primarily established for comparison of different filler metals. That is why the specified material properties are derived from all weld metal. Therefore, a standardized procedure [12, 13] exists, which describes how to establish all weld metals by arc welding. As the WAAM deposits are also all weld metals, similar chemical and mechanical properties of the manufactured components as given in the data sheets are expected.

In the following work, a comprehensive investigation of the developed microstructure has been conducted, the chemical and mechanical properties of the blade have been studied and compared with the values of the data sheet. Moreover, process-related properties like the surface condition and the macroscopic structure have been evaluated.

4.2 Surface condition

The achievable surface quality of WAAM based on CMT is quite smooth compared to the rough surface achieved with the standard GMAW process. Surface roughness measurements of the CMT blade showed a comparable roughness as achieved by sand casting, hot rolling, or flame cutting (see Fig. 4). The arithmetic average of around eight layers showed an absolute value (R_a) of 24.5 μm , and the average distance between highest peak and lowest valley (R_z) was measured with 135.3 μm .

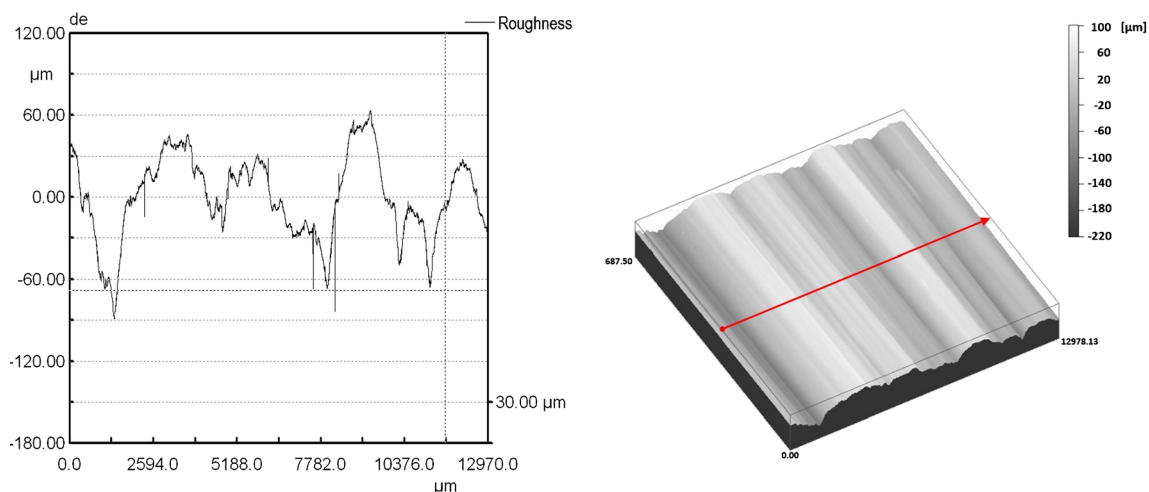
**Fig. 4** Linescan of absolute surface roughness (R_a) of CMT blade-like geometry (approx. eight layers)

Table 2 Chemical composition of welded sample in weight % compared to typical analysis [11, 17]

	C	Si	Mn	P	S	Cr	Mo	Ni	N	O
CMT-welded blade	0.037	0.50	1.43	0.017	0.004	22.10	2.94	8.52	0.16	0.041
Analysis solid filler wire	0.025	0.5	1.6	<0.03	<0.02	23.0	3.0	9.0	0.14	–

4.3 Chemical composition

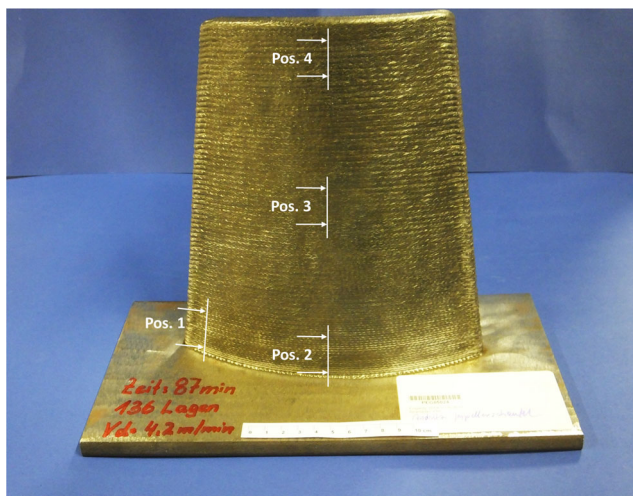
In Table 2, the chemical composition of the solid filler wire given in the data sheet is compared with chemical analysis of the blade-like component.

The alloy content of the weld seam is similar to the typical analysis stated in [11, 17]. The oxygen content is not specified in standards and data sheet, but the measured value of the blade, 410 ppm, is quite low and indicates that good toughness properties can be expected.

4.4 Metallographic investigation

The metallographic analysis offers a profound picture of the material quality of the component. The focus of this investigation was laid on porosity, abnormal microstructures, differences in the microstructure between bottom, mid and top area of the blade-like component as well as hardness profiles over several layers.

Four different areas containing each approximately eight layers in the blade-shaped geometry were selected and investigated (compare Fig. 5). The view is orthogonal to the welding direction. Position 1 (Pos. 1) represents the welding start-area. Position 2 (Pos. 2) is also located on the first eight welded layers but in the middle of the blade. Position 3 (Pos. 3) covers a cross section in the medium height of the blade and position 4 (Pos. 4) is situated on the upper layers.

**Fig. 5** Location of specimens for microstructural investigation

Hardness investigations have been conducted to ensure the homogeneity of the layer-by-layer welded seam as well as to preclude possible hardening/softening effects. Two hardness profiles (Pos. 1 and Pos. 2) starting in the base material (unalloyed steel) and covering approximately the first five layers are shown in Fig. 6. Constant hardness levels in both positions with mean hardnesses in the weld area of 266 HV on Pos. 1 and 270 HV on Pos. 2 are identified. These hardness values fit to the typical hardness range of duplex stainless steel weld metals of 240–320 HV₁₀ [14] and no hardening or softening has been detected. The hardness of the unalloyed steel base plate was 180–210 HV and no hardening in the heat affected zone was found.

Although it is well known that the applied horizontal welding position is in general not prone to pore formation or lack of fusion, a closer look was done on polished specimens using light optical microscopy (LOM) and scanning electron microscopy (SEM). No indications for porosity or lack of fusion, but a considerable number of non-metallic, Si-Al-O containing inclusions, in sizes up to 1 μm were observed (Fig. 7). Only a few inclusions in the range 1–4 μm were detected. Similar results were found in all positions (Pos. 1, 2, 3, and 4). However, such types of inclusions are typical for GMAW weld metals and are small slag particles.

The macrostructure of the four different positions is shown in Fig. 8. The single seam/multilayer structure is clearly visible, and a wall thickness between 8 and 10 mm can be attested. The layer thickness is around 1.5 mm. A macroscopic grain growth from the bottom via different layers to the top could be detected. This can be explained by the low welding speed and the reduced heat conduction caused by the thin wall structure which promotes a solidification direction almost perpendicular to the ground. Once solidified, this will be the basis for epitaxial grain growth which leads to these macroscopic visible structures.

In the cross section of positions 1 and 2, a full penetration in combination with a good wetting behavior of the first layer can be seen. Nevertheless, the amount of dilution with the base plate is low, which is a well-known feature of the CMT process. Responsible therefore is the high-frequency mechanical droplet detachment in combination with a minimized arc burning time [4, 5].

For the light optical investigations, a Beraha II etching agent (mixture of water, hydrochloric acid, ammonium bifluoride, potassium metabisulfite) was applied [15]. In Fig. 9, the resulting microstructures of the different cross sections (Pos. 1–4) are illustrated. A columnar-like grain growth

Fig. 6 Hardness profiles of cross section blade root area at **a** Pos. 1 and **b** Pos. 2

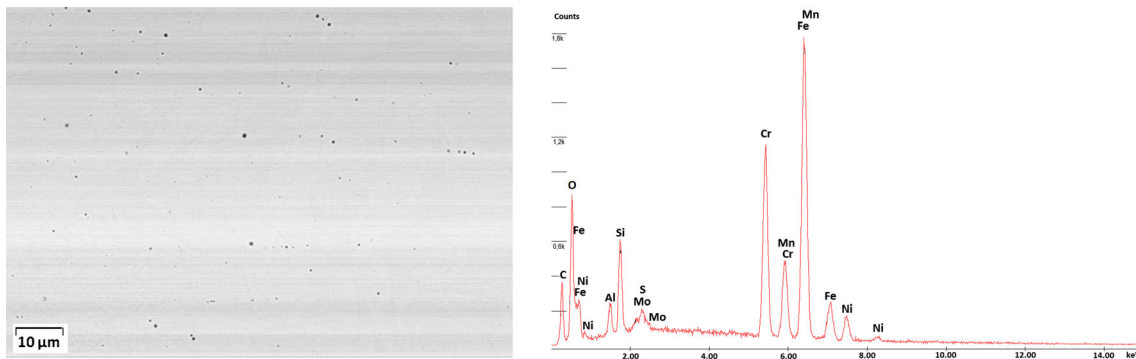
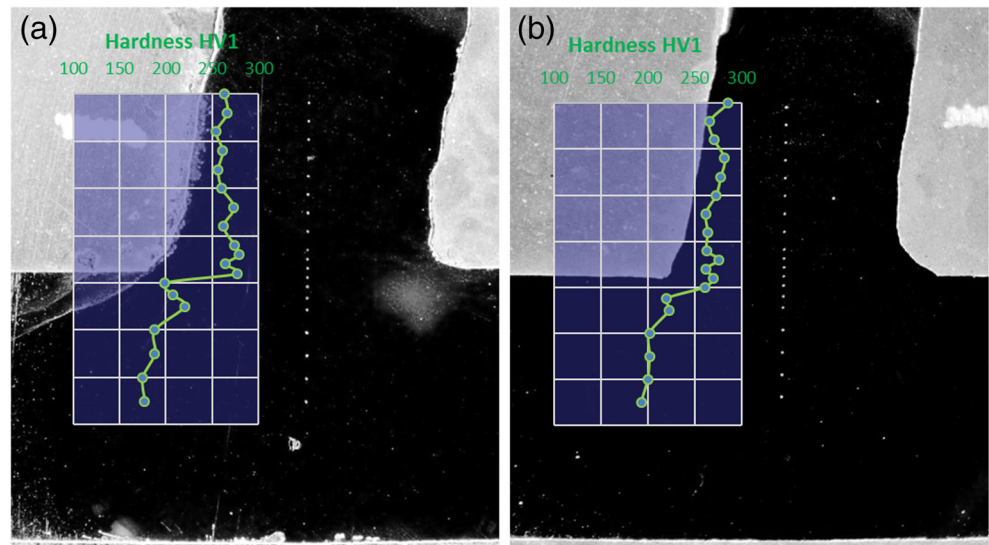


Fig. 7 SEM-investigation of polished surface (pos. 3) and EDX analysis of inclusions

is visible. Generally, the microstructure looks like a typical duplex stainless steel weld microstructure [14] with austenite (white) in a colored δ -ferrite matrix.

The first look at the duplex stainless steel weld metal microstructure of the CMT-MAM sample at lower magnification with light optical microscopy raised some concerns about “black areas” (see Fig. 10, left picture).

SEM examination at higher magnification, Fig. 10, right picture, identified the “black areas” as a very fine microstructure, but no porosity or undesirable phases were detected. This fine microstructure occurs mainly in the transition zone between two seams.

For identification of this very fine microstructure, further EBSD mode analysis was applied. Therefore, it was necessary

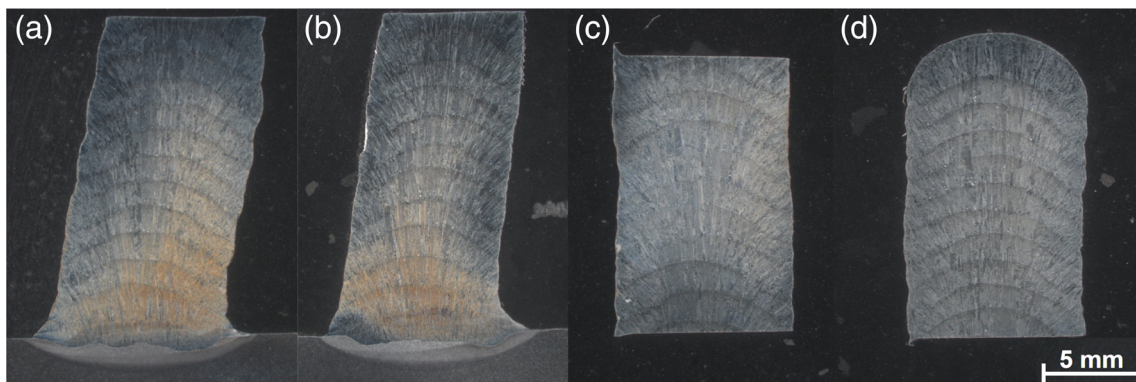
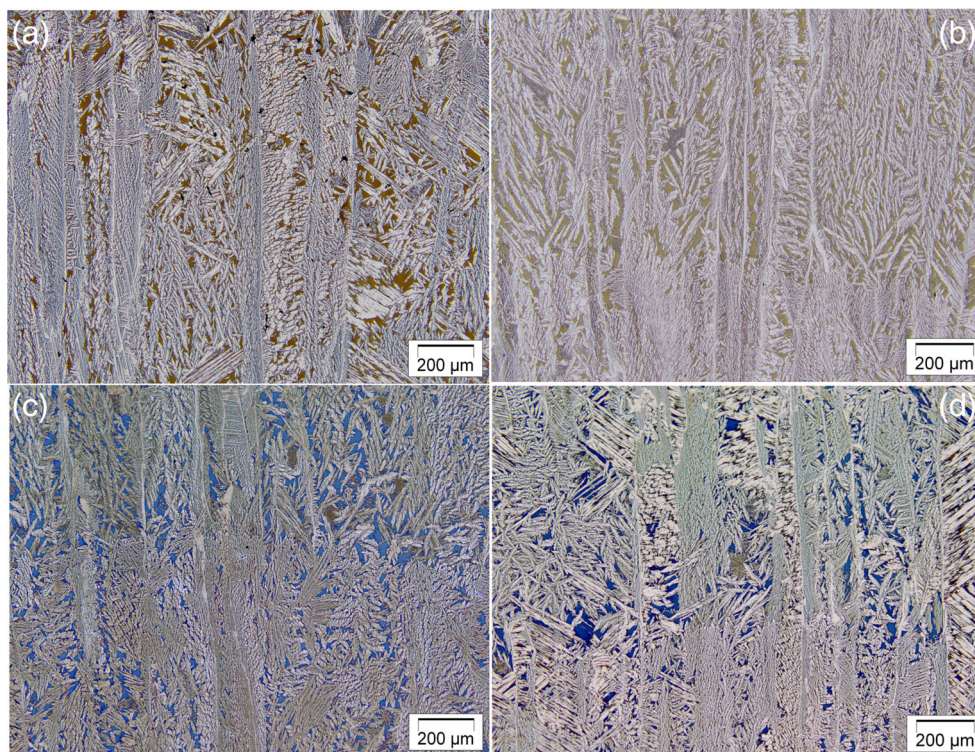


Fig. 8 V2A-etched macroscopic cross sections. **a** Pos. 1-welding start. **b** Pos. 2-first welded layers, blade middle. **c** Pos. 3-medium height, blade middle. **d** Pos. 4-upper layers, blade middle

Fig. 9 Microstructure in light optical investigations. **a** Pos. 1-welding start. **b** Pos.2-first welded layers, blade middle. **c** Pos. 3-medium height, blade middle. **d** Pos. 4-upper layers, blade middle



to improve the sample preparation to achieve acceptable EBSD measurements. After applying conventional mechanical polishing methods in a final preparation step, a focused ion beam, a so-called argon ion beam cross section polisher, was used to reveal a truly representative cross section of samples free of artifacts and distortion [16]. The tiny dark spots in Fig. 11 are related to this polishing technique. Using this sample preparation technique, the very fine microstructure (Fig. 10) could be identified by EBSD as secondary austenite (Fig. 11). The EBSD investigation also pointed out a preferred crystallographic orientation of the δ -ferrite matrix in [001] direction—red colored, respectively, along the direction [001] \rightarrow [101]—orange colored. In contrast, the austenite crystallographic orientation shows different, more or less bloc wise orientations.

4.4.1 δ -ferrite content

The δ -ferrite content, measured on the cross section with a Feritscope, was in the range between 35 FN and 36 FN.

Moreover, a quantitative area analysis of an EBSD phase mapping of the microsection offered a ferrite content between 26 and 29% (see Fig. 12), which is converted to FN approximately 27–31 FN. However, the EBSD-calculated values are strongly influenced by the position of the microsection, the two-dimensional view as well as the magnification used for establishing the color coded maps, what may be the reason for the slightly different results. However, these values are on the lower limit for duplex stainless steel welds, what is explainable by the reduced heat transmission caused by the thin blade wall which results in a progressed diffusion-controlled transformation of δ -ferrite in austenite.

4.5 Mechanical properties

For technical applications, reliable mechanical and technological properties of the manufactured component within certain limits are required. From the development of arc welding

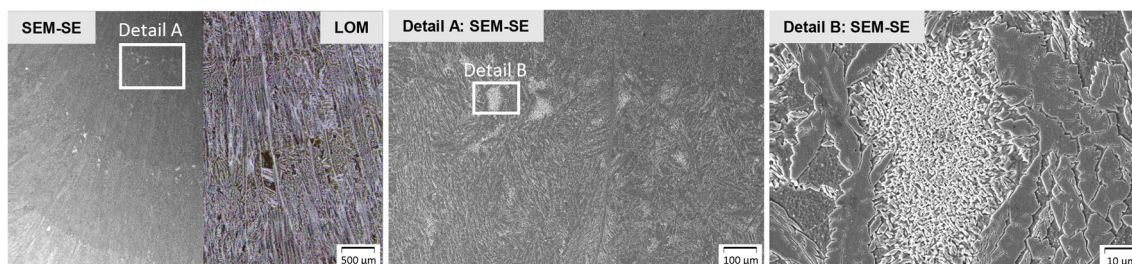


Fig. 10 Microstructure investigation “black areas” (Pos. 2)

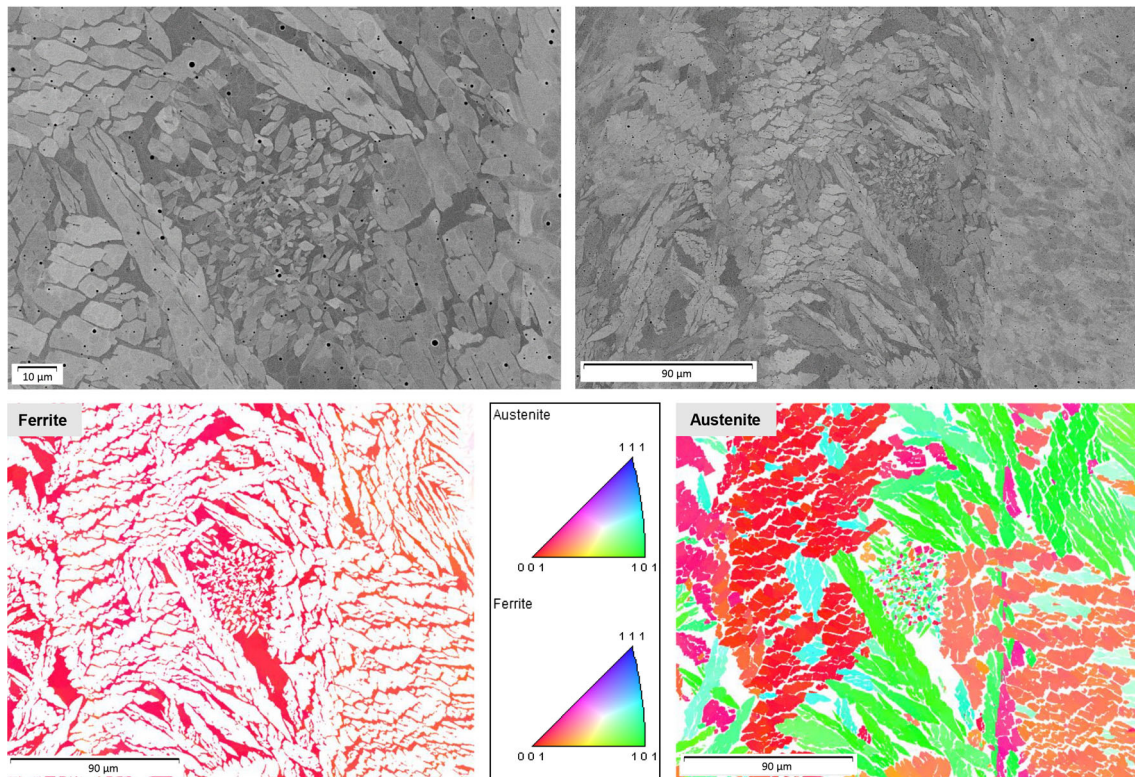


Fig. 11 EBSD-microstructure identification of “LOM black spots”; colored phase is named in the left upper corner of the picture

duplex stainless steel filler metals, it is well known that the most challenging requirements are often related to toughness and/or porosity issues. As the filler metals for CMT are the same as for GMAW, they are already designed for the highest weld quality. Also the influences of different shielding gases on weld metal properties are very well understood [18, 19].

To evaluate the mechanical properties of the CMT blades, tensile and toughness tests have been conducted. In Fig. 13, the location of the samples for mechanical testing is shown.

ISO-V toughness testing was done at room temperature in longitudinal and transversal weld direction using Charpy subsized samples according to EN 148-1. Due to the curved structure, the maximal producible sample size for longitudinal and transversal direction was different. The sample length was

kept to 55 mm and the height was 10 mm. However, the thickness was subsized: for transversal samples 7.5 mm and for longitudinal samples 5 mm. Moreover, the location of the 2-mm deep V-notch of the longitudinal test samples have been selected: in notch position “transition zone,” the notch tip was placed in the heat affected zone of a seam, and in notch position “seam,” it was placed in the middle of a seam, which is shown in the cross section in Fig. 12. Table 3 shows the results of the toughness test.

The impact strength of the blade is nearly the same under all conditions, independent on the examination area. Only the location of the notch in case of longitudinal testing has a marginal influence on the variation. When the notch is placed in the middle of the seam, in the columnar microstructure, the deviation is slightly increased. However, a calculation based

Fig. 12 EBSD—color coded mapping for determination of ferrite and austenite on two positions (a, b)

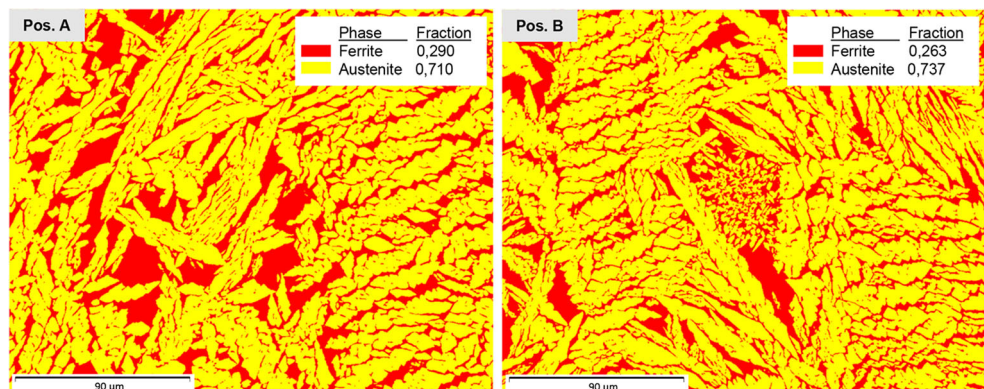
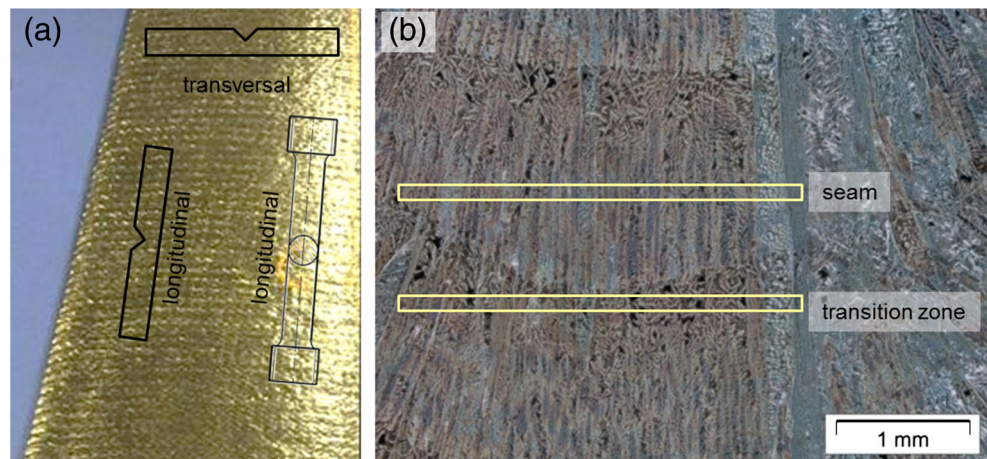


Fig. 13 Location of **a** Charpy- and tensile test specimens. **b** Position of notch in relation to the microstructure



on their impact strength showed that all toughness values are in general high compared to around 100 J achieved with standard ISO-V specimen size (10 × 10 × 55 mm) as stated in the filler metal data sheet.

Three tensile test specimens, according to DIN 50125—special geometry with a size $\varnothing 6 \times 30$ mm, were tested according to DIN EN 6892-1 at room temperature. The test area was in transverse weld direction, which is different to the test area of all-weld test samples for filler metal data sheets, where the examination area is in longitudinal direction of the weld. The measured values of yield strength ($R_{p0.2}$, $R_{p1.0}$), tensile strength (R_m), Young's modulus (E), elongation (A ; $L_0 = 5d_0$) and reduction in area (Z) in comparison to data sheet values are given in Table 4. The results of the tensile tests are homogeneous with a very moderate standard deviation and quite similar to the values described in the data sheet. Differences in yield strength could be subjected to the different measurement directions (transversal vs. longitudinal) caused by a different grain orientation.

5 Summary

Metal additive manufacturing is at the time one of the hot topics in the scientific landscape. From the economic point of view, wire arc additive manufacturing (WAAM) seems thereby to be a very interesting approach. The electric arc welding processes provide the necessary energy to melt metals within reasonable times, they use wires, and they are matured

joining technologies. A literature review pointed out that GMAW is already very successful in use over years for a layer-by-layer additive manufacturing technology for hydro-power Pelton runners. But also, the limitations get obvious: To manufacture thinner parts, it is necessary to run GMAW on a very low energy level to prevent a melt down of already deposited and solidified metal, but then the process tends to get unstable and heavy spatter occurs.

Several years ago, a modified, low energy GMAW short arc process, CMT (Cold Metal Transfer), was developed for joining steel to aluminum. The core of this development is a very stable, high-frequency mechanical forward and backward movement of the filler wire which allows a significant reduction of the arc burning time and a smooth, energy-reduced metal transfer. Features, which are also essential for WAAM. For this reason, this application-related study was initiated to evaluate the capabilities of CMT in respect to additive manufacturing and to determine the mechanical behavior of additive manufactured duplex stainless steel blades. Therefore, simplified blades were build up layer-by-layer using a commercial available duplex stainless steel filler wire. Afterwards, surface condition, microstructure, and mechanical properties were analyzed. The achieved surface roughness was comparable to sand castings respectively hot rolled surfaces. The chemical composition of the blade was comparable to the analysis given by the filler metal data sheet. Additionally, the measured oxygen content was low, which indicates good toughness properties. The microstructure was comparable to conventional GMAW duplex stainless steel weld metals: An austenite/ δ -

Table 3 Results of ISO-V toughness tests at room temperature

		Charpy size	Absorbed energy	Impact strength	
	Sample position	Notch position	[mm]	[J]	[J/cm ²]
CMT blade	Transversal		55 × 10 × 7.5	77 ± 3.3	129 ± 5.9
	Longitudinal	Transition zone	55 × 10 × 5	51 ± 3.4	129 ± 8.3
	Longitudinal	Seam	55 × 10 × 5	51 ± 5.2	128 ± 11.9
All weld metal	Transversal		55 × 10 × 10	70	~100

Table 4 Results of tensile tests at room temperature compared to data sheet [11]

	R _{p0,2} [N/mm ²]	R _{p1,0} [N/mm ²]	R _m [N/mm ²]	E [N/mm ²]	A [%]	Z [%]
Mean value	455	576	717	195	28	68
Data sheet	510	550	700	–	25	–

ferrite microstructure was revealed with a δ -ferrite content of 30FN. The δ -ferrite grains showed a preferred crystallographic orientation in [001] direction, whereas the austenite grains were bloc wise, randomly oriented. No indication for porosity and lack of fusion could be observed by the metallographic investigations. The mechanical properties were matchable to the values given in the filler metal data sheet.

This study has shown that CMT is capable for additive manufacturing due to already existing robotic interfaces, available welding technology and predefined parameter settings. Additionally, a big variety of filler wires is available, which is already metallurgical optimized for welding and approved for joining. The component surface smoothness can be remarkable improved and thinner walls can be realized compared to standard GMAW processes. By keeping the base of the layer-by-layer manufactured component horizontal, the 3D complexity is limited, but if the base is mounted on a turntable which allows an additional movement, much more complex geometries can be established.

It was also demonstrated in this study that at least down to 8–10 mm thin additive manufactured walls the mechanical properties are comparable to the properties of all weld metal stated in the data sheet. This also suggests the conclusion that WAAM components could be handled in respect to their mechanical properties like welds and the comprehensive available welding knowledge could be applied for optimization of their mechanical and metallurgical properties.

References

- Oesterreicher A, Wiener J, Roth M, Moser A, Gmeiner R, Edler M, Pinter G, Griesser T (2016) Tough and degradable photopolymers

- derived from alkyne monomers for 3D printing of biomedical materials. *Polym Chem* 7(Issue 32)
- Korzhik VN, Khaskin VY, Grinyuk AA, Tkachuk VI, Peleshenko SI, Korotenko VV, Babich AA (2016) 3D-printing of metallic volumetric parts of complex shape based on welding plasma-arc technologies. *The Paton Welding Journal* No. 5-6
- D Appelyard; *Welding Pelton Runners*, HRW-Hydro Review Worldwide (2012)
- Schweißpraxis aktuell: CMT-Technologie; Fronius Int. GmbH, WEKA Media GmbH (2013); ISBN 978-3-8111-6879-4
- Current Welding Practice CMT Technology; Fronius Int.; DVS Media GmbH (2014); ISBN 978-3-945023-36-5
- J. Bruckner, K. Himmelbauer; *Cold Metal Transfer—Ein neuer Prozess in der Fügetechnik*; DVS-Berichte Band 237; 2005
- Zhang H, Feng J, He P, Zhang B, Chen J, Wang L (2009) The arc characteristics and metal transfer behaviour of cold metal transfer and its use in joining aluminium to zinc-coated steel. *Mater Sci Eng A* 499(Issues 1–2)
- Pickin C, Williams S, Lunt M (2011) Characterisation of the cold metal transfer (CMT) process and its application for low dilution cladding. *J Mater Process Technol* 211(Issue 3)
- Williams S, Martina F, Adison A, Ding J, Pardal G, Colegrove P (2016) Wire + arc additive manufacturing. *Mater Sci Technol* 32(Issue 7)
- Übersicht der Prozessregelvarianten des MSG-Schweißens; Merkblatt DVS 0973, DVS Media GmbH, Düsseldorf, 2014
- Data sheet “Thermanit 22/09”; www.boehler-welding.com, 2014
- ISO 15792-1 (2011) Welding consumables—test methods—Part 1: test methods for all-weld metal test specimens in steel, nickel and nickel alloys
- EN ISO 15792-1 (2012) Schweißzusätze - Prüfverfahren - Teil 1: Prüfverfahren für Prüfstücke zur Entnahme von Schweißgutproben an Stahl, Nickel und Nickellegierungen
- van Nassau L, Meelker H, Hilkes J (1993) Welding duplex and super-duplex stainless steels. *Welding in the World* 31(5)
- Petzow G (1994) *Metallographisches Ätzen*; Gebr. Bornträger, Berlin
- N. Erdmann, R. Campell, S. Asahina; *Precise SEM cross section polishing via argon beam milling*; *Microscopy Today*, 2006
- EN ISO 14343 -A (2009) Welding consumables—wire electrodes, strip electrodes, wires and rods for arc welding of stainless and heat resisting steels—classification”
- Valiente Bermejo MA, Karlsson L, Svensson L-E, Hurtig K, Rasmuson H, Frodigh M, Bengtsson P (2015) Effect of shielding gas on welding performance and properties of duplex and superduplex stainless steel welds. *Welding in the World* 59(2)
- Valiente Bermejo MA, Karlsson L, Svensson L-E, Hurtig K, Rasmuson H, Frodigh M, Bengtsson P (2015) Effect of welding position on properties of duplex and superduplex stainless steel circumferential welds. *Welding in the World* 59(5)